N94-10593

# Squeezed States of Electrons and Transitions of the Density of States

Seung Joo Lee
*Department of Physics, Korea Military Academy*
*Seoul, 199-799, Korea*

Chung In Um
*Department of Physics, Korea University*
*Seoul, 136-701, Korea*

**Abstract**

Electron systems which have low dimensional properties have been constructed by squeezing the motion in zero, one or two-direction. An isolated quantum dot is modelled by a potential box with delta-profiled, penetrable potential walls embedded in a large outer box with infinitely high potential walls which represent the work function with respect to vacuum. We show the smooth crossover of the density of states from the three-dimension to quasi-zero-dimensional electron gas.

## 1 Introduction

Quantum wires and quantum boxes with three-dimensionally confined electrons constitute a considerable part of recent semiconductor research [1, 2]. To study the optical properties of these systems, one should investigate the density of states (DOS) carefully, because the change in the density of states affects directly the optical properties of these structures as a result of reduced dimensionality.

The DOS of a low dimensional electron gas(LDEG) in the presence of magnetic field has been discussed in many literatures measuring the magnetocapacitance [3, 4]. Furthermore an electrical confinement which is usually controlled by (alternate) gate voltage [5] and, so called the illumination method [6] are used to get a LDEG. The etched silicon filaments also discussed recently as quantum wires or quantum dots [7]. But the DOS of a LDEG of confined electrons in small space which is constructed by reducing the size of the confinement is not discussed frequently, see ref. [1]. A typical example of an ideal system having Q0D charactor is that of electron confined in a quantum box with impenetrable potential barriers. Despite of the large number of studies on quantum wire and quantum box structures up to date, we have not found research on the crossover of the DOS from a three dimensional DOS to a quasi-zero dimensional DOS. In Section 2, to illustrate the formation of a quasi-one-dimensional electron gas(Q1DEG) using the classical electrostatic method, a simple metal-insulator-semiconductor(MIS) structure

with very many parallel gate electrodes has been treated by making use of the conformal mapping method. In section 3, we consider a rather artificial quantum box structure, so called the three directional double-barrier resonant-tunneling structures(DBRTS) to study quantum mechanically, and have calculated the local density of states and the global density of states. In section 4, the crossovers of the DOS is calculated. Especially, we reveal the crossovers of the DOS from 3D to Q0D.

## 2 Construction of the very many parallel quantum wires

To study electrical properties of a quantum wire, we first start with a quasi-two-dimensional electron gas(Q2DEG) at simple metal-insulator- semiconductor(MIS) structure. A Q2DEG system with many parallel gate electrodes is shown in Fig.1 in which an electron gas is confined to the x-z plane. We actually try to confine the electrons in the z-direction as well to form a Q1DEG system.

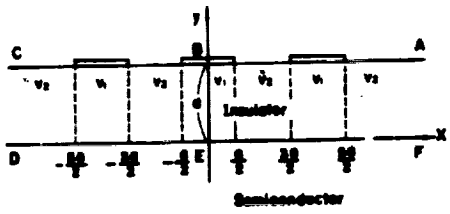


Fig.1

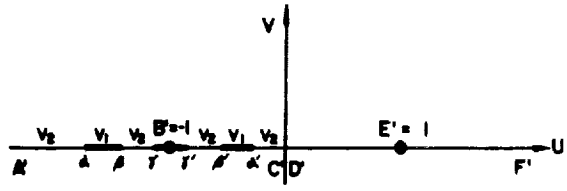


Fig.2

Fig.1 A Structure of symetric gate arrays. Fig.2 The boundary condition in w-plane.

To calculate the charge(density) distribution at the MIS interface (y=0 plane) to see the formation of a Q1DEG, we will use the conformal mapping method which is useful especially for two-dimensional problems and we assume that significant changes in the electrode potential (and thus is density in the channel) cause only a slight change in the near junction band bending. This type of approximation has been used by Shik [8] to calculate various properties of the MIS structure.

The problem is solving the Laplace equation in insulator region.

$$\frac{\partial^2 \Psi}{\partial x^2} + \frac{\partial^2 \Psi}{\partial y^2} = 0 \tag{1}$$

with the boundary condition;

At $y = d$, $\Psi\ |_{y=d}$ is alternate gate potential $V_1$ and $V_2$ and at $y = 0$, $\Psi\ |_{y=0}$ is constant, i.e. equipotential surface. The next step is getting the distribution of the surface carrier density.

$$n_s(x) = \frac{K_d}{4\pi e}\frac{\partial \Psi}{\partial y}\ |_{y=0}\ . \tag{2}$$

We solve the problem by taking the following conformal transformation [9].

$$W = U + iV = e^{\pi z/d}, z = x + iy$$

where $d$ is the thickness of the insulator, Now the insulator region is mapped on the upper half plane and the boundary condition is given as in Fig.2.

After getting the potential which satisfy the boundary condition, we now get the electron density distribution $n(x)$ analytically from Eq.(2):

$$\begin{aligned} n(x) \ = \ & \frac{K_d V_2}{4\pi e}[1 + (V_1/V_2)^{-1}\sum_{n=1}^{m}(-1)^{n+1} < \sinh((2n-1)\pi a/2d) \\ & [\cosh(\pi x/d) + \cosh((2n-1)/2d)] >] \end{aligned} \tag{3}$$

where $a$ is the gate interval and $m$ is the number of gates.

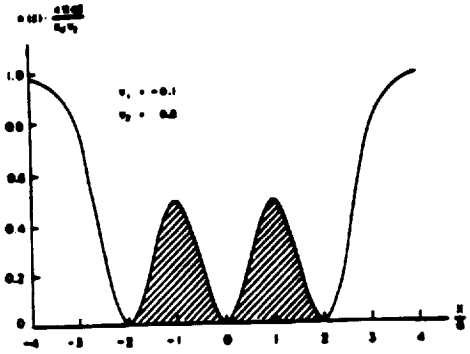

Fig.3

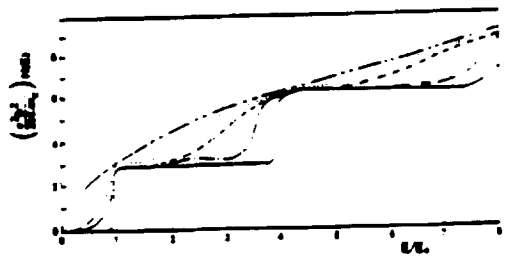

Fig.4

Fig.3 The surface charge density vs. position.

Fig.4 Crossover of the global DOS from 3D to 2D in the range $U_1 = 0$ to $U_1 = 20$, as a function of $E/E_0$. Here $U_1$ takes the values 0, 2, 12, 16, 20.

A typical density distribution is illustrated in Fig.3 where we can see immediately the many parallel Q1DEG (eventhough we show here only two wires). The one dimensional electron density of the order of $10^6/cm$ is obtained for the typical operating gate voltage when $a$ is 1000Å. We also investigated the case of anti-symmetric gate voltage. Similar results have been obtained but in symmetric case it is easy to construct one dimensional electron channels especially for smaller number of gates. In our calculation we took $a/d = 1$, which satisfy the first approximation, $y = 0$ plane is equipotential.

# 3 The quantum box model and the DOS

Now we come back to quantum system with a delta-profiled quantum box. Usually a quantum dot is an element of the array of quantum dots. But the interaction among quantum dots decreases rapidly with increasing dot separation [10] and is unimpotant for the usual experimental situation [11].

Therefore a separated single quantum box is taken for our study. For a rectangular wire($L_{y(z)} \ll \lambda_D$), Arora and others[12] used the impenetrable potential walls, but in this paper we consider three sets of penetrable barriers. We start our calculations with the model, i.e., the typical three directional DBRTS, which consists of two thin($\sim 50\mathring{A}$)$Al_xGa_{1-x}As$ layers, separated by a thin GaAs layer along all three directions. The potential is expressed by

$$V(x,y,z) = V_1\delta(x+a) + \delta(x-a) + V_2\delta(y+b) + \delta(y-b) + V_3\delta(z+c) + \delta(z-c). \tag{4}$$

In this potential, the six $Al_xGa_{1-x}As$ potential barriers have been replaced by $\delta$-functions with strengthes $V_1, V_2$ and $V_3$ in the $x, y$, and $z$ direction, respectively. The parameters $V_i (i = 1,2,3)$ are given by

$$V_i = d_i \Delta V_{ci} \tag{5}$$

where $d_i$ are the barrier widths and $\Delta V_{ci}$ are the conduction-band discontinuities. In order to deal with finite density of states,[13], we must place our structure in a large impenetrable rigid box extending from $-L/2$ to $L/2$. With proper boundary conditions[14], the Schrödinger equation is separable. we can write the wave function in the product form

$$\Psi(r) = \psi(x)\psi(y)\psi(z) = \prod_{i=1}^{3} \Psi_i \tag{6}$$

The separated wave functions, $\Psi_i$, satisfy the reduced equations.

$$\Psi_i'' + [2m_e/\hbar^2][E_i - V_i]\Psi_i = 0 \tag{7}$$

with

$$E = \sum_{i=1}^{3} E_i \tag{8}$$

Here $E$ is the total energy corresponding to the Hamiltonian H and $E_i (i = x,y,z)$ is the energy eigenvalue of $\Psi_i$.

The local density of states in the DBRTS has been obtained in various cases [15]. It is defined as a function of $\mathbf{r} = (x,y,z)$ and $E$ by

$$\begin{aligned} N(x,y,z;E) &= -(2/\pi) Im G(\mathbf{r},\mathbf{r}';E) \\ &= 2\sum_{\alpha\beta\gamma}\sum_{k_x}\sum_{k_y}\sum_{k_z} |\Psi_{\alpha k_x}(x)|^2 |\Psi_{\beta k_y}(y)|^2 |\Psi_{\gamma k_z}(z)|^2 \delta(E - E_k), \end{aligned} \tag{9}$$

where the factor of 2 implies spin degeneracy, $G(\mathbf{r},\mathbf{r}';E)$ is the single particle Green's function, and $\alpha, \beta$, and $\gamma (= e$ or $0)$ label state parity. Next we consider the global DOS $N(E)$. It can be calculated by taking the integration over the box volume,

$$N(E) = 8\int_0^a dx \int_0^b dy \int_0^c dz N(x,y,z;E). \tag{10}$$

The amplitude of the wave function inside the well for both even and odd parities of $x, y$, and $z$ componenets are given elsewhere[14]. $N(E)$ can be rewritten as follows:

$$\begin{aligned} N(E) &= (2/\pi^3)\int_0^\infty dp_1[G_e(p_1)+G_o(p_1)+(G_e(p_1)-G_o(p_1))\sin(2p_1)/2p_1] \\ &\times \int_0^\infty dp_2[G_e(p_2)+G_o(p_2)+(G_e(p_2)-G_o(p_2))\sin(2p_2)/2p_2] \\ &\times \int_0^\infty dp_3[G_e(p_3)+G_o(p_3)+(G_e(p_3)-G_o(p_3))\sin(2p_3)/2p_3]\delta(E-E_k). \end{aligned} \quad (11)$$

The properties of functions $G_e(p_i)$ and $G_o(p_i)$ are already revealed in Ref.14.

When we take appropriate limiting cases, the Eq.(11) recovers all the well-known expressions of the DOS of 3D, 2D, 1D, and 0D. since the calculations are straightforward, we haven't repeated here.

# 4 Crossovers of the density of states

Now we consider crossovers of the global DOS from a high dimension to a low dimension.

## 4.1 From 3D to 2D

This case may happen when two of three potentials $U_i$'s(see the reference 15) approach zero, while the remainder varies from zero, i.e., 3D case, to infinity, i.e., 2D case. The Eq.(11) can be modified as

$$\frac{2\pi}{4bc}\frac{\hbar^2}{2m_c}N(E) = \int_0^{\pi/2(E-E_o)^{1/2}} dp_1[G_e(p_1)+G_o(p_1)+(G_e(p_1)-G_o(p_1))\sin(2p_1)/2p_1] \quad (12)$$

The result of the numerical behavior of Eq.(12) is shown in Fig.4 and indicates the transition of the DOS from 3D to 2D. In this case we take $U_2 = U_3 = 0$, $U_1$ changes from 0 to 20, and $E/E_o$ varies from 0 to 8. Higher values of $U_1$ correspond to a staircase-like 2D behavior which shows steps at $E/E_o = l^2$ with $l = 1, 2, 3, \cdots$.

## 4.2 From 2D to 1D

This corresponds to the case of $U_3$ going to zero, $U_1$ to infinity, and $U_2$ varying from zero, i.e., 2D case, to infinity, 1D case. So $G(p_3) = 1, G_e(p_1) = \pi\sum\delta(p_1-(l+1/2)\pi), G_o(p_1) = \pi\sum\delta(p_1-(l+1)\pi)$. Then we can get the modified equation of N(E) as follows ;

$$\begin{aligned} \frac{\pi^2\hbar^2}{4cm_c}N(E) &= \sum_{m=0}^{\infty}\int_0^{\pi/2(E-E_o)} dp_2[G_e(p_2)+G_o(p_2)+(G_e(p_2)-G_o(p_2))\sin(2p_2)/2p_2] \\ &\times [1/[(\pi/2a)^2E/E_o-((m+1/2)\pi/a)^2-(p_2/b)^2]^{1/2} \\ &+ 1/[(\pi/2a)^2E/E_o-(m+1)\pi/a^2-(p_2/b)^2]^{1/2}]. \end{aligned} \quad (13)$$

The Fig.5 shows the graphical result, that is, the crossover of the global DOS from 2D to 1D. In this case, for the sake of convenience, we take $a = b, U_3 = 0$ and $U_1 \to \infty, U_2$ takes the values

of 0, 2, 8, 16, 20, and $E/E_o$ is taken from 0.0 to 8.0. One can see that the steps at $E/E_o$ = 1, 4, 9, $\cdots$, that is, the two dimensional band edges, are shifted to peaks at $E/E_o$ = 2, 5, 8, 10, $\cdots$, i.e., the one dimensional band edges. As $U_2$ increases, the motion of confined electrons along the $y$ axis atarts to shrink and is guided only along the $z$ axis. This weak additional confinement shifts the 2D band edges towards higher energies and finally the typical 1D characteristics of the DOS comes to bevisualized. Higher values of $U_2$ correspond to increased sharp peaks of the DOS of the 1-D quantum wire case, which are in good agreement with those of Arakawa and Sakaki [13] and of Tsang [16]. The values at $E/E_o$ = 5 and 10 are roughly twice those at $E/E_o$ = 2 and 8, respectively, which comes from the double degeneracy of the eigenstates. Similar discussions were treated by Berggrent and Newson [17] in the case of the 2D electrons in the presence of a magnetic field.

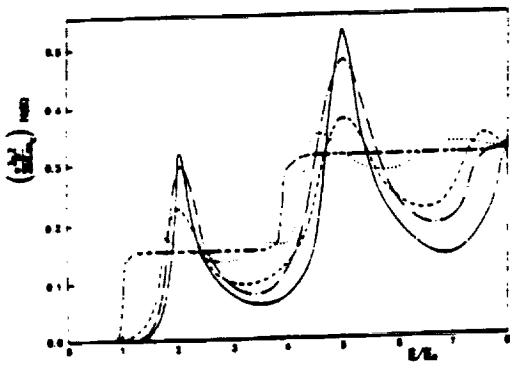

Fig.5

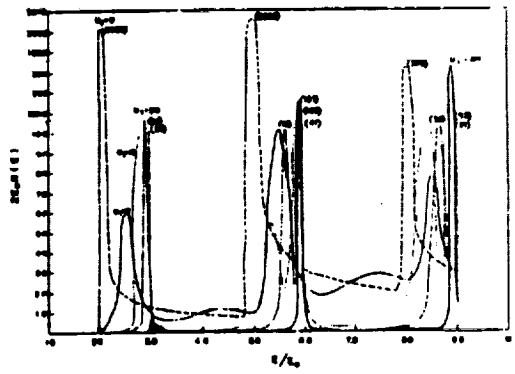

Fig.6

Fig.5 Crossover of the global DOS from 2D to 1D. Here we take $U_1 = \infty and U_2$ = 0, 2, 8, 16, 20. Higher values of $U_2$ correspond to a sawtoothlike 1D behavior.

Fig.6 Crossover of the global DOS from 1D to 0D. Here we take $U_1 = U_2 = \infty$ and $U_3$ = 0, 2, 10, 20, 80. Higher values of $U_3$ correspond to a sharp line shape 0D behavior.

## 4.3 From 1D to 0D

In this case, we take both $U_1$ and $U_2$ to be infinity, and $U_3$ vary from zero, 1D case, to infinity, 0D case. Then Eq.(11) becomes

$$N(E) = (2/\pi)\sum_{l,m=1}^{\infty}\int_0^{\pi/2(E/E_o)^{1/2}} dp_3[G_o(p_3)+G_o(p_3)+(G_o(p_3)-G_o(p_3))\sin(2p_3)/2p_3] \times \delta[E-(\hbar^2/2m_c)(l\pi/2a)^2+(m\pi/2b)^2+(p_3/c)^2 \quad (14)$$

$$(2E_o)N(E) = \sum_{l,m=1}^{\infty}\frac{G_o(t)+G_o(t)+(G_o(t)-G_o(t))\sin(2t)/2t}{[E/E_o-l^2-m^2]^{1/2}} \quad (15)$$

where $t = (\pi/2)(E/E_o - l^2 - m^2)^{1/2}$.

Fig.6 shows the transition of the global DOS from 1D to 0D. For the sake of convenience, we put $a = b = c$. The Eq.(15) recovers the well-known DOS of a quantum dot [16], when we take $U_3$ to be infinity. Sawtooth type maximums at $E/E_o = 2, 5, 8, 10, \cdots$, are now moved to the positions at $E/E_o = 3, 6, 9, 11, \cdots$, as the strength of $U_3$ increases. When the confining potential increase, both primary peaks and secondary ones appear, which reflect the coexistance of 1D and 0D behavior. The secondary peak with the lower energy is a reminescence of the 1D DOS shifted towards higher energy due to the additional confinement, and the primary peak (higher energetic peak) arises from quasi 0D states. Bacause the differences between peaks are so high, we used different scales for the DOS axis ranging from 1.0 to over 2000. The DOS clearly shows the potential strength ($U_i$) dependence of the spatial quantization through $E_o$. This kind of secondary peaks are also shown in many experimental data of a transport measurement [18]. We know that the electron systems used in above experiments are in an intermediate state between 1D and 0D, because the potential strengths are not infinitely high.

We believe that this kind of DOS transition which shows intermediate states will also occur in real systems where, for example, the barriers have finite widths. For barriers with finite thickness, the effective mass of the electron changes in passing from the quantum-well region (GaAs) to the barrier regions (AlGaAs) of the structure. Bruno and Bahder [15] have considered this for the one directional DBRTS case and showed that the DOS at the low-energy subband edges is higher than the DOS at the same energies in the absences of barriers (for delta-profiled barriers). In our case, we can estimate that our result for the DOS will be increased a bit upward at the same energies because of the additive form of the potential which we have taken.

In this paper, first we showed as an example the formation of many electron wires using the conformal mapping method. Next, considering a penetrable quantum box, with a volume of a $axbxc$, in a very large rigid box of volume $L^3$, we calculated the general form of the local and global DOS.

The merit of this model is as follows :

1) the model is simple to handle and easy to calculate analytically,

2) in this model, one can recover the results of all the limiting cases of the 3D, 2D, 1D, and 0D,

3) starting from one equation we can discuss all three crossover cases.

# 5 Acknowledgments

This work is supported by the Thermal and Statistical Physics Center of the Korea Science and Engineering foundation and the ETRI, KTA of the Ministry of Telecommunication, Korea.

# References

[1] See, for example, R. R. Gerhardts, D. Weiss, and K. v. Klitzing, Phys. Rev. Lett. **62**, 1173(1989); Scientific American, July 1991, p86.

[2] U. Merkt, J. Huser, and M. Wagner, Phys. Rev. B43, 7320 (1991); K. Kern, D. Heitmann, P. Grambow, Y. H. Zhang, and K. Ploog, Phys. Rev. Lett. 66, 1618(1991); A. Kumar, S. E. Laux, and F. Stern, Phys. Rev. B42, 5166(1990).

[3] T. P. Smith, B. B. Goldberg, P. J. Stiles, and M. Heiblum, Phys. Rev. B32, 2696(1985).

[4] V. Mosser, D. Weiss, K. v. Klitzing, K. Ploog, and G. Weimann, Solid State Commun. 58, 5(1986).

[5] C. W. J. Beenakker and H. van Houten, Solid State Physics 44, 1(1991).

[6] R. R. Gerharts, D. Pfannkuche, D. Weiss, and U. Wulf, in *High Magnetic Fields in Semiconductor Physics III*, Springer Series in Solid State Science edited by G. Landwehr (Springer-Verlag Berlin, 1991).

[7] L. T. Canham, Appl. Phys. Lett. 57, 1046(1990).

[8] A. Y. Shik, Sov. Phys. Semicond. 19, 463(1985).

[9] H. Kober, "Dictionary of Conformal Representations" Dover Publications, Inc., 1952.

[10] T. Demel, D. Heitmann, P. Grambow, and K. Ploog, Phys. Rev. Lett. 64, 788(1990).

[11] V. Gudmundsson and R. R. Gerhardts, Phys. Rev. B43, 12098 (1991)

[12] V. K. Arora and M. Prasad, Phys. Stat. Sol. (b) 117, 127 (1983); H. Z. Zheng, H. P. Wei, D. C. Tsui and G. Weinmann, Phys. Rev. B34, 5635(1986); P. F. Yuh and L. L. Wang, Appl. Phys. Lett. 49, 1738(1986).

[13] Y. Arakawa and H. Sakaki, Appl. Phys. Lett. 40, 939 (1982).

[14] S. J. Lee, N. H. Shin, and J. J. Ko, J. of Kor. Phys. Soc., 24, 197(1991).

[15] J. D. Bruno and T. B. Bahder, Phys. Rev. B39, 3657(1989).

[16] W. T¿ Tsang, Semiconductors and Semimetals, 24, 397(1987), Academic Press.

[17] K. F. Berggrent and D. J. Newson, Semicond. Sci. Technol. 1, 327(1986).

[18] T. P. Smith *III*, Surf. Sci. 229, 239(1990).